

Frequency resonance in Josephson-junction arrays under strong driving

Jong Soo Lim,¹ M.Y. Choi,^{1,2} and Beom Jun Kim³

¹*Department of Physics, Seoul National University, Seoul 151-747, Korea*

²*Korea Institute for Advanced Study, Seoul 130-012, Korea*

³*Department of Molecular Science and Technology, Ajou University, Suwon 442-749, Korea*

We study resonance behavior of a two-dimensional fully frustrated Josephson-junction array driven by high alternating currents. The signal-to-noise ratio (SNR) is examined as the frequency of the driving current is varied; revealed is a certain frequency range where the SNR is enhanced. Such resonance behavior is explained by considering the dynamic order parameter at zero temperature. We also compute the work, which corresponds to the Ohmic dissipation of the energy due to external currents, and discuss its possibility as a measure of stochastic resonance.

PACS numbers: 74.81.Fa, 74.40.+k, 05.40.-a

Conventionally, the stochastic resonance (SR) stands for the phenomenon that a weak signal can be amplified and optimized by the assistance of noise. The SR, in general requiring three basic ingredients, i.e., an energetic activation barrier or a form of threshold, a coherence input (such as periodic driving), and a source of noise, has been observed in a variety of systems.¹ It has also been investigated in the regime of strong periodic driving.^{2,3} In particular, Pankratov² considered fluctuation dynamics of a Brownian particle in a quartic potential subject to strong periodic driving, and studied the SR behavior reflected in the signal-to-noise ratio (SNR) at given driving amplitude, as the frequency and the noise intensity are varied. The observed enhancement of the SR behavior in a certain range of the driving frequency, which may be called *frequency resonance* for convenience, was explained in terms of the very weak dependence of the mean transition time on the noise intensity in that frequency range. From the practical viewpoint, such characteristic behavior is important in systems with many degrees of freedom, which constitute many devices operating in the strong driving regime. Among interesting systems with many degrees of freedom is the two-dimensional (2D) fully frustrated Josephson-junction array (FFJJA), which grants a direct experimental realization and provides rich dynamics.^{4,5,6} Recent study includes dynamic transitions as well as SR in FFJJAs driven by uniform alternating currents.⁷ However, responses to strong driving with the possibility of frequency resonance have not been examined in a system with many degrees of freedom including the FFJJA.

This work examines the FFJJA driven by high alternating currents, with attention paid to the frequency resonance behavior. In order to describe the dynamic responses, we consider the staggered magnetization, the average of which defines the dynamic order parameter, and compute its power spectrum. As manifested by the corresponding SNR, the system indeed exhibits frequency resonance: the SR-like behavior as the driving frequency is varied. It is discussed in view of the variation of the zero-temperature states with the driving frequency. In addition, we also obtain the work performed by the driving currents and explore the possibility as a new measure

of the resonance behavior.⁸

We begin with the equations of motion for the phase angles $\{\phi_i\}$ of the superconducting order parameters on the grains forming an $L \times L$ square lattice. Within the resistively-shunted-junction model under the fluctuating twist boundary conditions (FTBC),⁹ we have

$$\sum_j' \left[\frac{d\tilde{\phi}_{ij}}{dt} + \sin(\tilde{\phi}_{ij} - \mathbf{r}_{ij} \cdot \Delta) + \eta_{ij} \right] = 0, \quad (1)$$

where the primed summation runs over the nearest neighbors of grain i and the abbreviations $\tilde{\phi}_{ij} \equiv \phi_i - \phi_j - A_{ij}$ and $\mathbf{r}_{ij} \equiv \mathbf{r}_i - \mathbf{r}_j$ with $\mathbf{r}_i = (x_i, y_i)$ denoting the position of grain i have been used. The thermal noise current η_{ij} satisfies $\langle \eta_{ij}(t)\eta_{kl}(t') \rangle = 2T\delta(t-t')(\delta_{ik}\delta_{jl} - \delta_{il}\delta_{jk})$ at temperature T in units of J/k_B with the Josephson coupling strength J . Note that \mathbf{r}_{ij} for nearest neighboring grains is a unit vector since the lattice constant has been set equal to unity throughout this paper. We have also expressed the energy and the time in units of $\hbar I_c/2e$ and $\hbar/2eRI_c$, respectively, with the critical current $I_c \equiv 2eJ/\hbar$ and the shunt resistance R . While in the FTBC the phase variables observe the periodic boundary conditions, the dynamics of the twist variables $\Delta \equiv (\Delta_x, \Delta_y)$ is governed by the equations

$$\begin{aligned} \frac{d\Delta_x}{dt} &= \frac{1}{L^2} \sum_{\langle ij \rangle_x} \sin(\tilde{\phi}_{ij} - \Delta_x) + \eta_{\Delta_x} - I_0 \sin(\Omega t) \\ \frac{d\Delta_y}{dt} &= \frac{1}{L^2} \sum_{\langle ij \rangle_y} \sin(\tilde{\phi}_{ij} - \Delta_y) + \eta_{\Delta_y}, \end{aligned} \quad (2)$$

where $\sum_{\langle ij \rangle_a}$ denotes the summation over all nearest neighboring pairs in the $a (= x, y)$ direction, η_{Δ_a} satisfies $\langle \eta_{\Delta_a}(t + \tau)\eta_{\Delta_{a'}}(t) \rangle = (2T/L^2)\delta(\tau)\delta_{a,a'}$, and the oscillating current $I_0 \sin(\Omega t)$ is injected in the x direction. In the Landau gauge, the bond angle A_{ij} , given by the line integral of the vector potential, takes the values

$$A_{ij} = \begin{cases} 0 & \text{for } \mathbf{r}_j = \mathbf{r}_i + \hat{\mathbf{x}}, \\ \pi x_i & \text{for } \mathbf{r}_j = \mathbf{r}_i + \hat{\mathbf{y}}. \end{cases}$$

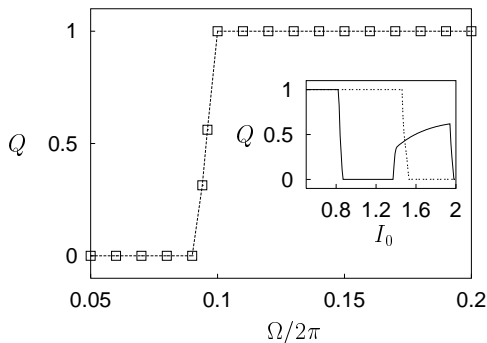


FIG. 1: Dynamic order parameter Q versus frequency Ω at zero temperature, for driving amplitude $I_0 = 1.2$ in the system of size $L = 16$. Inset : Q versus I_0 for $\Omega/2\pi = 0.06$ (solid line) and $\Omega/2\pi = 0.12$ (dotted line).

For the study of the dynamic behavior, associated with the Z_2 symmetry in the FFJJA, it is convenient to consider the chirality

$$C(\mathbf{R}, t) \equiv \text{sgn} \left[\sum_{\mathbf{P}} \sin \left(\tilde{\phi}_{ij}(t) - \mathbf{r}_{ij} \cdot \mathbf{\Delta}(t) \right) \right] \quad (3)$$

and the staggered magnetization

$$m(t) \equiv \frac{1}{L^2} \sum_{\mathbf{R}} (-1)^{x_i+y_i} C(\mathbf{R}, t), \quad (4)$$

where $\sum_{\mathbf{P}}$ denotes the directional plaquette summation of links around the dual lattice site $\mathbf{R} \equiv \mathbf{r}_i + (1/2)(\hat{\mathbf{x}} + \hat{\mathbf{y}})$. The dynamic order parameter is then given by the staggered magnetization averaged over one period of the oscillating current:⁷

$$Q \equiv \frac{\Omega}{2\pi} \left| \oint m(t) dt \right|. \quad (5)$$

Unlike in Ref. 7, we keep the driving amplitude fixed at the value larger than the critical one (mostly $I_0 = 1.2$) and probe the behavior as the frequency Ω is varied.

In the numerical calculation, the set of the equations of motion in Eqs. (1) and (2) are integrated via the modified Euler method with time steps of size $\Delta t = 0.04$. We have varied the step size, only to find no essential difference. Typically, data have been taken after the initial 500 driving periods, which have turned out to be long enough to achieve proper stationarity. In addition, 500 independent runs have been performed, over which the average has been taken.

The behavior of the dynamic order parameter Q with the driving amplitude I_0 was investigated, revealing that at zero temperature the dynamically ordered state ($Q > 0$) and the disordered one ($Q = 0$) appear alternatively as I_0 is raised (see the inset of Fig. 1).⁷ Here we examine how Q changes as the driving frequency Ω is varied for

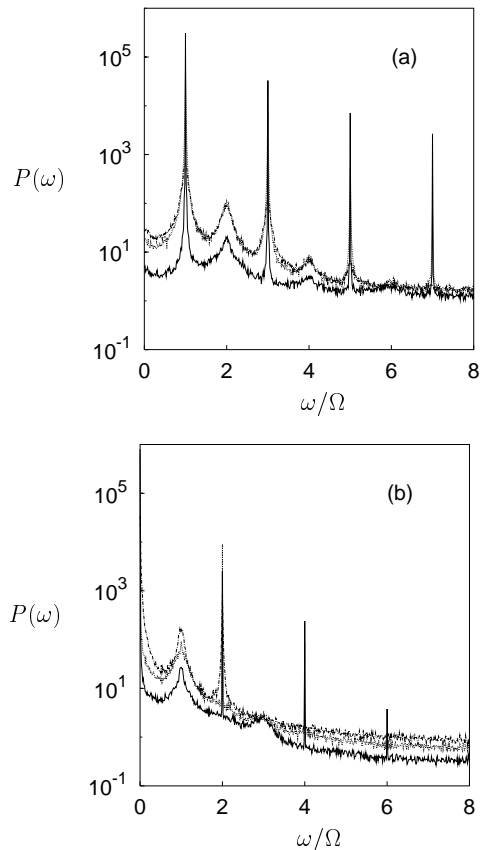


FIG. 2: Power spectrum $P(\omega)$ of the staggered magnetization in the system of size $L = 16$, driven with the amplitude $I_0 = 1.2$ and the frequency $\Omega/2\pi =$ (a) 0.06 and (b) 0.12. The temperature is given by $T = 0.1, 0.2,$ and 0.3 from below.

fixed I_0 and display the result in Fig. 1. Such behavior of Q with Ω can be understood as follows: At low driving frequencies, the external current changes with time more slowly than the intrinsic dynamics and thus the system has enough time to follow the external driving. Consequently, the two ground-state configurations of the chirality alternate in time, leading to the oscillation of the staggered magnetization $m(t)$. From the definition of the dynamic order parameter, this in turn results in $Q = 0$. On the other hand, for larger values of Ω , the system cannot change the staggered magnetization in time since the driving changes too fast in comparison with the intrinsic time scale, and there follows $Q = 1$.

We next investigate the resonance behavior, focusing on the power spectrum of the staggered magnetization and its SNR defined to be

$$\mathcal{R} = 10 \log_{10} \left[\frac{S}{N} \right]. \quad (6)$$

The signal S represents the peak power intensity at the driving frequency Ω while the background noise level N is estimated by the average power spectrum around the

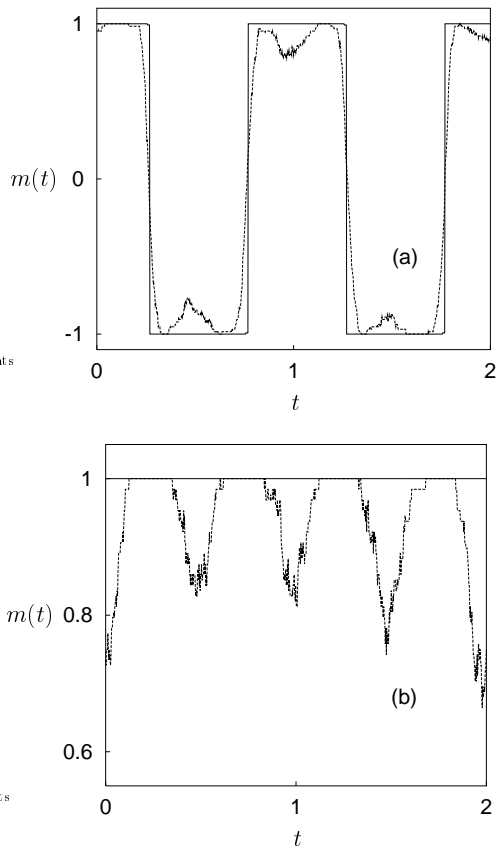


FIG. 3: Time evolution of the staggered magnetization $m(t)$ for driving amplitude $I_0 = 1.2$ and frequency $\Omega/2\pi =$ (a) 0.06 and (b) 0.12. The temperature is given by $T = 0$ (solid line) and 0.1 (dotted line); time t in the horizontal axis is expressed in units of the period $2\pi/\Omega$.

signal peak.

In Fig. 2, we display typical behavior of the power spectrum $P(\omega)$ at low temperatures $T = 0.1, 0.2$, and 0.3 in the presence of the driving current with amplitude $I_0 = 1.2$ and frequency $\Omega/2\pi =$ (a) 0.06 and (b) 0.12. Note the substantial difference in the behavior of $P(\omega)$ at $\Omega/2\pi = 0.06$ and at $\Omega/2\pi = 0.12$: In the former $P(\omega)$ exhibits pronounced peaks at odd harmonics ($\omega = \Omega, 3\Omega, 5\Omega, \dots$), whereas even harmonics instead of odd ones are pronounced in the latter. Somewhat similar features were also observed in the opposite case that the amplitude is varied with the frequency kept fixed.⁷

This interesting difference between slow and fast driving is manifested by the zero-temperature behavior of the staggered magnetization, shown Fig. 3: At low driving frequencies such as $\Omega/2\pi = 0.06$, the staggered magnetization exhibits periodic oscillations in perfect accord with the external driving at zero temperature, generating pronounced odd harmonics. As thermal noise is introduced here, the sharp peaks at odd harmonics are gradually suppressed while broad peaks at even harmonics emerge.

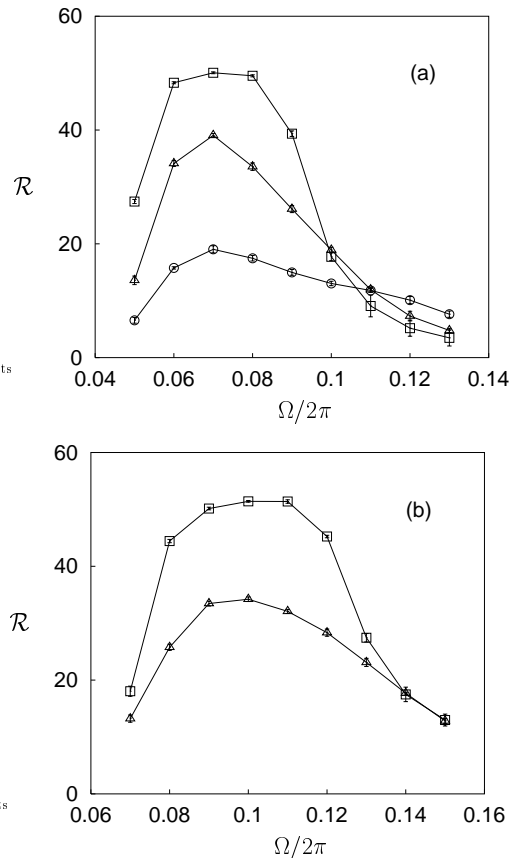


FIG. 4: Behavior of the signal-to-noise ratio \mathcal{R} with the driving frequency Ω , measured in the system of size $L = 16$ at the driving amplitude $I_0 =$ (a) 1.2 and (b) 1.6. Included in (a) are data at temperature $T = 0.1, 0.2$, and 0.3 while in (b) $T = 0.1$ and 0.2 (from top to bottom). Error bars are less than the size of symbols and lines are merely guides to eyes.

On the other hand, at high frequencies the system cannot follow the external driving so that even harmonics are prominent. The peak at $\omega = 0$ for $\Omega/2\pi = 0.12$ reflects the nonzero value of Q , i.e., the nonzero time-average value of $m(t)$.

Figure 4 shows the SNR versus the driving frequency at the amplitude $I_0 =$ (a) 1.2 and (b) 1.6. As the frequency Ω is increased, the SNR first increases, reaches its maximum at frequency Ω_R , which we call the resonance frequency, and then decreases with further increase of Ω . Such characteristic behavior can again be explained by considering the zero temperature behavior: At low driving frequencies, we have $Q = 0$ since $m(t)$ oscillates between 1 and -1 at zero temperature. As the frequency Ω is increased, the driving current changes with time rapidly, making the system reside more in the out-of-equilibrium state. Since in equilibrium vortices stay at positions where the lattice pinning potential is minimum,¹⁰ the increase of Ω can be interpreted as the effective reduction in the barrier due to the lattice pin-

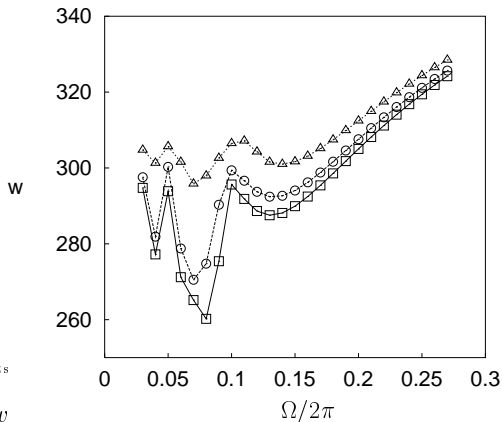


FIG. 5: Work (per site) done by the driving current, as a function of the frequency Ω , in the system of size $L = 8$. The driving amplitude is given by $I_0 = 1.2$ and the temperature $T = 0.05, 0.10$, and 0.20 from below.

ning potential. Accordingly, the escape from the potential well occurs more easily, leading to the increase of the SNR, as shown in Fig. 4. Beyond the resonance frequency Ω_R , however, further increase of Ω suppresses the SNR since there is not enough time to escape from the potential well. This argument is also supported by Fig. 4(b), where for comparison the behavior of the SNR at the amplitude $I_0 = 1.6$ is shown. It is observed that the resonance frequency Ω_R shifts toward higher values, which is easily understood in view of that the escape from the well occurs at a higher frequency for a larger value of I_0 . Note also that the maximum value of the SNR decreases with the temperature.

It was proposed that the work done by the external driving can be used as a quantitative measure to detect SR; indeed the work as a function of temperature has been shown to have maximum near the SR temperature T_{SR} ⁸. Such resonant behavior was explained by the increase of the work as the resonant response is enhanced. In this section, we investigate the work W done by the external driving current in the FFJA:

$$\begin{aligned}
 W &= -\frac{I_0\Omega}{n} \int_{t_0}^{n\mathcal{T}+t_0} \left\langle \sum_y (\phi_{0,y} - \phi_{N,y}) \cos(\Omega t) \right\rangle dt \\
 &= \frac{I_0}{n} \int_{t_0}^{n\mathcal{T}+t_0} \langle V \sin(\Omega t) \rangle dt, \quad (7)
 \end{aligned}$$

where $\mathcal{T} \equiv 2\pi/\Omega$ is the period of the driving current, $\langle \dots \rangle$ denotes the ensemble average, and the time-average is taken during n periods of driving current. To obtain the second line, we have integrated by parts and used the Josephson relation $V = (\hbar/2e)(d\phi/dt)$. The same equation can also be derived from the Ohmic dissipation [with the power $V(t)I(t)$ at time t] averaged over n periods.

In Fig. 5, we display how the work per site $w \equiv L^{-2}W$ changes with the frequency Ω . Unexpectedly, the work does not exhibit any resonant behavior, in sharp contrast with the result in Ref. 8. We presume that this discrepancy results from the following fact: While the work in Ref. 8 is related to the position of the Brownian particle, the voltage V giving the work in Eq. (7) corresponds to the velocity of a vortex rather than the position. It is thus not likely that the work serves as an appropriate measure to quantify frequency resonance in our system.

In summary, we have studied dynamic properties of the 2D FFJA driven uniformly by alternating currents, with attention paid to the frequency resonance phenomena in the strong driving regime. For this purpose, we have computed the power spectrum of the staggered magnetization and the corresponding SNR. It has been shown that there exists a certain frequency range where the SNR is enhanced. Such behavior may be understood in view of the variation of the zero-temperature states with the driving frequency. Direct experimental observation of these dynamic properties is presumably possible with the state-of-art vortex imaging technique.¹¹ In addition, we have calculated the work done by the driving current, and probed its possibility as a new quantitative measure of resonance. It has been found that the work does not display any resonant behavior, suggesting inadequacy as a measure of resonance.

This work was supported in part by the BK21 Program, the SKOREA Program (M.Y.C.), and the KOSEF Grant No. R14-2002-062-01000-0 (B.J.K.).

¹ See, e.g., L. Gammaitoni, P. Hänggi, P. Jung, and F. Marchesoni, *Rev. Mod. Phys.* **70**, 223 (1998).

² A.L. Pankratov, *Phys. Rev. E* **65**, 022101 (2002).

³ M.C. Mahato and S.R. Shenoy, *Phys. Rev. E* **50**, 2503 (1994); J.C. Phillips and K. Schulten, *ibid.* **52**, 2473 (1995); F. Apostolico, L. Gammaitoni, F. Marchesoni, and S. Santucci, *ibid.* **55**, 36 (1997); M.C. Mahato and A.M. Jayanavar, *Physica A* **248**, 138 (1998); M. Thorwart and P.

Jung, *Phys. Rev. Lett.* **78**, 2503 (1997); A.L. Pankratov and M. Salerno, *Phys. Lett. A* **273**, 162 (2000).

⁴ K.K. Mon and S. Teitel, *Phys. Rev. Lett.* **62**, 673 (1989); J.S. Chung, K.H. Lee, and D. Stroud, *Phys. Rev. B* **40**, 6570 (1989); S. Kim and M.Y. Choi, *ibid.* **48**, 322 (1993); H.J. Luo, L. Schülke, and B. Zheng, *Phys. Rev. Lett.* **81**, 180 (1998).

⁵ V.I. Marconi and D. Domínguez, *Phys. Rev. Lett.* **87**,

- 017004 (2001).
- ⁶ G.S. Jeon, H.J. Kim, M.Y. Choi, B.J. Kim, and P. Minnhagen, Phys. Rev. B **65** 184510 (2002).
- ⁷ G.S. Jeon, J.S. Lim, H.J. Kim, and M.Y. Choi, Phys. Rev. B **66** 024511 (2002).
- ⁸ T. Iwai, J. Phys. Soc. Jpn. **70**, 353 (2001)
- ⁹ B.J. Kim, P. Minnhagen, and P. Olsson, Phys. Rev. B **59**, 11506 (1999).
- ¹⁰ C.J. Lobb, D.W. Abraham, and M. Tinkham, Phys. Rev. B **27**, 150 (1983); M. Yoon, M.Y. Choi, and B.J. Kim, *ibid.* **61**, 3263 (2000).
- ¹¹ See, e.g., A. Tonomura, et al., Nature (London) **397**, 308 (1999).